

The Effect of Zinc Doped Bismuth Ferrite on Changes in Structural and Microwave Absorption Properties through the Sol-gel Synthesis Method

Suharno Wira Sukarsa^{1*}, Bambang Soegiyono², Sri Budiawanti¹

¹Department of Physics Education, Faculty of Teacher Training and Education, Universitas Sebelas Maret, Surakarta 57126, INDONESIA

²Department of Physics, Faculty of Mathematics and Natural Science, Universitas Indonesia, Depok 16424, INDONESIA

*Corresponding Author

DOI: <https://doi.org/10.30880/ijie.2022.14.02.011>

Received 30 April 2021; Accepted 10 September 2021; Available online 02 June 2022

Abstract: The zinc (Zn) doped bismuth ferrite (BiFeO₃) have been successfully synthesized through the sol-gel autocombustion method as a microwave absorbent material through a composite process with silicone rubber. The characterizations of zinc doped bismuth ferrite nanoparticles was done using the X-ray diffraction (XRD), the Fourier transform infrared (FTIR), the vibration sample magnetometer (VSM), and the vector network analyzer (VNA). Through the XRD test, the nanoparticle BiFe_{1-x}Zn_xO₃ (x = 0, 0.06, and 0.12) have a crystal structure of rhombohedral R3c. Through the FTIR test, it was observed that the area of wave number 491–569 cm⁻¹ were used as an absorber for BiFeO₃, while the one in zinc doped BiFeO₃ were observed to be 489–636 cm⁻¹. The VSM test shows that the BiFe_{1-x}Zn_xO₃ nanoparticles (x = 0, 0.06, and 0.12) have ferromagnetic properties and potentially change to paramagnetic properties with the addition of zinc doping. The VNA test were obtained, bismuth ferrite without doping has a reflection loss (RL) of -25.79 dB with a narrower frequency range and bismuth ferrite with zinc doping (% wt x = 0.12) has a RL of -30.02 dB with a wider frequency range so that zinc doped BiFeO₃ potentially to be a good absorbent material.

Keywords: Nanocrystalline, bismuth ferrite, sol gel, rhombohedral, microwave absorption

1. Introduction

The absorption of microwaves originated from the radar development innovation in World War II. Therefore, in its development. The microwave absorbent materials are used for the development of stealth or anti-detection aircraft. The microwave absorbing materials have been prepared to coat the airframe of fighter aircraft [1]. For anti-detection technology, microwave absorption was at X band frequency because it was suitable for the military world, especially missile anti-detection technology.

In line with the development of anti-detection material technology, materials engineering has been carried out to produce microwave absorbent materials. The multiferroic materials as bismuth ferrite material was that simultaneously have ferromagnetic and ferroelectric properties [2], [3]. The multiferroic materials that have electric and magnetic properties were simultaneously interesting to study, because multiferroic materials are potential to have good electromagnetic wave absorption [4-6]. The during its development, ferrite-based absorbent was made as a magnetic material. The absorption of microwaves on magnetic materials of barium hexaferrite-epoxy composites [7]. The manufacture of carbon-based silencers as nonmagnetic materials has also been widely used and the study of microwave

*Corresponding author: suharno_71@staff.uns.ac.id

2022 UTHM Publisher. All rights reserved.

penerbit.uthm.edu.my/ojs/index.php/ijie

absorption properties on carbon based [8]. The research conducted through a combination of magnetic materials and non-magnetic materials was a composite Fe/Carbon [9].

The innovation of BiFeO₃ synthesis employs various methods such as solid-state reaction [10]. The chosen synthesis technique was the sol-gel autocombustion method because it has better homogeneity, has efficient energy, has a low temperature, and capable of producing nano-sized particles. The selection of doping zinc into Bismuth ferrite was expected to affect changes in crystal structure properties, magnetic properties, and microwave absorption properties. The zinc doped BiFeO₃ potentially contribute in improving ferroelectric properties.

In this research, the synthesis method of bismuth ferrite with sol-gel autocombustion to obtain nanocrystalline was going to be reported. Furthermore, characterization was carried out to determine changes in crystal structure and changes in microwave absorption properties due to zinc doping.

2. Material and Methods

The synthesis of the BiFe_{1-x}Zn_xO₃ nanocrystals (% wt, x = 0, 0.06, 0.12) have been successfully carried out using the sol-gel autocombustion procedure. The Fig. 1 shows the synthesis of bismuth ferrite by the sol gel autocombustion procedure. The synthesis of bismuth ferrite doping zinc were carried out by mixing a stoichiometric solution of Bi(NO₃)₃.5H₂O, Fe(NO₃)₃.9H₂O, and Zn(NO₃)₂.6H₂O. The solution mixture was stirred on a hotplate using a magnetic stirrer for 2–3 hours under stable heated of 80 °C until gel was produced. The sol occurs during the process of mixing the solution and heated as a wet chemical process with the addition of citric acid C₆H₈O₇. The gel was obtained after mixing the brown and clear solution. After obtained the gel, the thermal properties were measured to determine the mass dropping temperature of bismuth ferrite doping zinc. Furthermore, the gel was heated as a dried process at a temperature of 150 °C for 1 hour, according to the results of the thermal analysis. The powders nanocrystalline of bismuth ferrite doping zinc were obtained after drying, grinding as a grounded process, and annealing at a temperature of 750 °C for 5 hours. The samples obtained in this study were BiFe_{1-x}Zn_xO₃ (% wt, x = 0, 0.06, and 0.12).

The BiFe_{1-x}Zn_xO₃ nanocrystals, x = 0, 0.06, and 0.12 were tested using the X-ray diffraction (XRD) Type Phillips PW 1710 at a diffraction angle of 2θ = 20–70° to determine the crystal structure of the samples. The fourier transformation infrared (FTIR) spectrum studies with a PerkinElmer type were measured at a wave number 350–4500 cm⁻¹. The magnetic properties of the samples were measured using the VSM type OXFORD VSM 1.2H and the microwave absorption properties of BiFe_{1-x}Zn_xO₃, (% wt, x = 0, 0.06, and 0.12) nanocrystals were measured using VNA type R3770 at the X band frequency (8.2–12.4 Ghz).

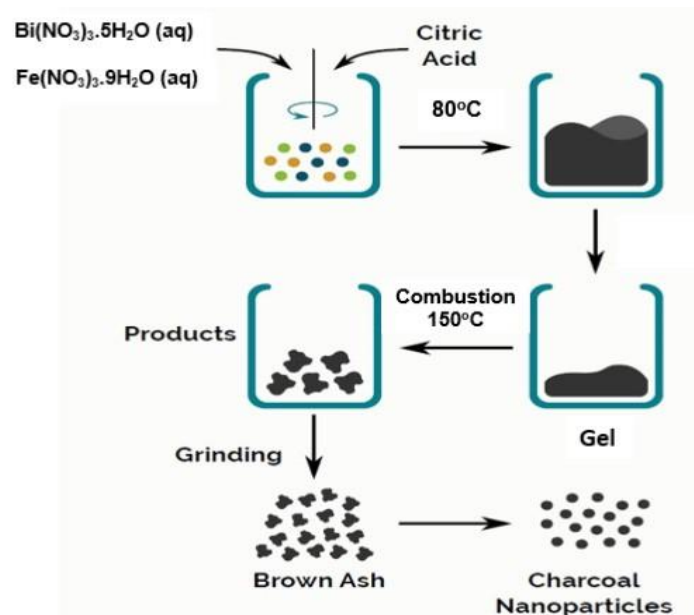


Fig. 1 - The synthesis of bismuth ferrite with sol-gel autocombustion method

3. Results and Discussion

3.1 Crystal Structure

The crystal structure were known through XRD test. The test result shows that the nanoparticle material of BiFe_{1-x}Zn_xO₃, (x = 0, 0.06, and 0.12) have a diffraction pattern, as shown in Fig. 2. The crystal structure analysis using Fullprof, samples of BiFe_{1-x}Zn_xO₃, (x = 0, 0.06, and 0.12) have a crystal system of rhombohedral space group R3c and the diffraction peak of *hkl* (012), (110), (104), (202), (024), (116), (122), (214) and the lattice parameters as shown in the

Table 1. The crystallite size (D) of $\text{BiFe}_{1-x}\text{Zn}_x\text{O}_3$, ($x = 0, 0.06, \text{ and } 0.12$) can be calculated using the Debye-Scherrer formula and obtained were 63.75 nm, 60.27 nm, 56.99 nm. This suggests that a decrease in crystal size due to zinc doping have the potential to change magnetic properties and microwave absorption properties [11].

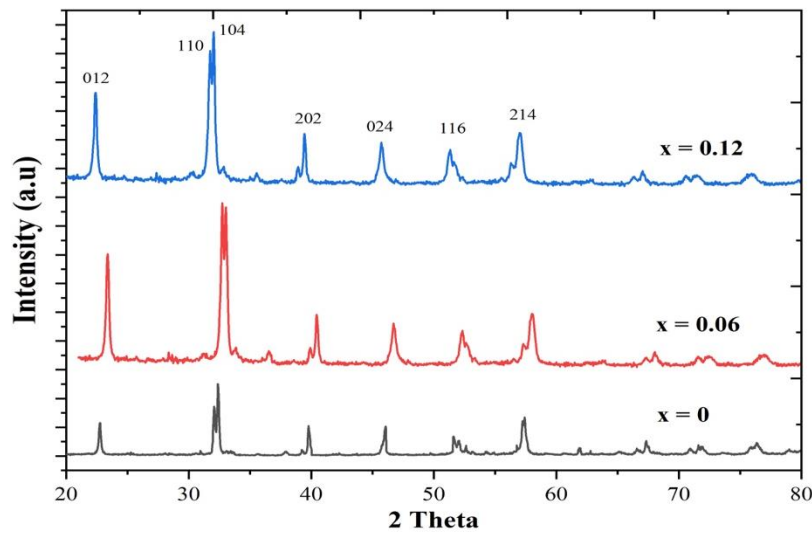


Fig. 2 - The X-ray diffraction pattern of $\text{BiFe}_{1-x}\text{Zn}_x\text{O}_3$ nanocrystals ($x = 0, 0.06, \text{ and } 0.12$)

Table 1 - The lattice parameters of $\text{BiFe}_{1-x}\text{Zn}_x\text{O}_3$ nanocrystals ($x = 0, 0.06, \text{ and } 0.12$)

Parameters	$x = 0$	$x = 0.06$	$x = 0.12$
$\alpha = \beta, \gamma$	$90^\circ, 120^\circ$	$90^\circ, 120^\circ$	$90^\circ, 120^\circ$
$a = b(\text{\AA})$	5.57830	5.62790	5.61610
$c(\text{\AA})$	13.8552	13.9109	13.8765
Volume (\AA^3)	373.3727	381.5711	373.1126

From Figure 2, its were observed that at substitutions $x = 0.06$ and 0.12 there were a shift in the top lattice plane (012) in the angle of $2\theta = 22^\circ$ and (110), (104) in the angle of $2\theta = 32^\circ$. The scrape of the top position was due to changes in lattice parameters or distortion lattice due to Zn ions²⁺ substitute the Fe ion³⁺ where was the Zn atom (1.35 Å) has a smaller atomic radius than the Fe atom (1.40Å) which were analyzed referring to the Bragg equation (Eq. (1) and Eq. (2)):

$$\sin \theta = \frac{n\lambda}{d_{hkl}} \tag{1}$$

$$\frac{1}{d_{hkl}^2} = \frac{h^2+k^2+l^2}{a^2+b^2+c^2} \tag{2}$$

At an angle of 32° , the addition of Zn doping of $x = 0-0.12$ into the Fe atom shows that the top positions of the lattice planes (110) and (104) are still split, which indicates that there were no change in the crystals structure of the rhombohedral space in group R3c. It can be concluded that the addition of zinc doping with the substitution of $x = 0.06-0.12$ did not change the rhombohedral crystal structure.

3.2 The FTIR Study

The Fig. 3 shows the FTIR spectrum of $\text{BiFe}_{1-x}\text{Zn}_x\text{O}_3$ ($x = 0, 0.06, \text{ and } 0.12$) were measured at room temperature with wavenumbers $350-4500 \text{ cm}^{-1}$. The FTIR spectrum of Zn doped BiFeO_3 have almost the same characteristics as BiFeO_3 , but the peak of the BiFeO_3 absorbent without Zn doping were smaller than the peak of Zn doped BiFeO_3 absorption. The results of the $\text{BiFe}_{1-x}\text{Zn}_x\text{O}_3$ spectrum ($x = 0, 0.06, \text{ and } 0.12$) were observed that on wavenumbers $400-600 \text{ cm}^{-1}$ have the characteristics as a metal oxide bond. In the figure, its were also observed that in BiFeO_3 on wave number $491-569 \text{ cm}^{-1}$ was the absorbent area, while in Zn doped BiFeO_3 were observed to be $489 - 636 \text{ cm}^{-1}$. In the wave

number 400–700 cm^{-1} area, bending vibration of Fe-O bonds occurs in the octahedral group FeO_6 and also the octahedral structure of BiO_6 [12], there was Fe-O stretching and H_2O Absorbance. The optimum absorber on BiFeO_3 was observed at the 539 cm^{-1} peak as stretching Fe-O and another peak at 402 cm^{-1} as bending vibration and both of them were characteristic of the octahedral FeO_6 group in perovskite compounds. The optimum absorption of Zn doped BiFeO_3 was observed at a peak of 539 cm^{-1} as stretching Fe-O and another peak at 402 cm^{-1} as bending vibration and both are characteristic of the octahedral FeO_6 group in perovskite compounds. In the area of wave number 3260–3654 cm^{-1} was the anti-symmetry and stretching symmetry of the H_2O and OH^- group bonds and the peak of 3445 was the peak of stretching. The 1555 cm^{-1} peak was associated with bending vibration H_2O and the peak of 1384 cm^{-1} corresponds to a condensation reaction in the process of sol formation due to the presence of citric acid [13]. It can be concluded that due to Zn doped BiFeO_3 , there were a change in the absorption peak but still in the region of relatively the same wave number.

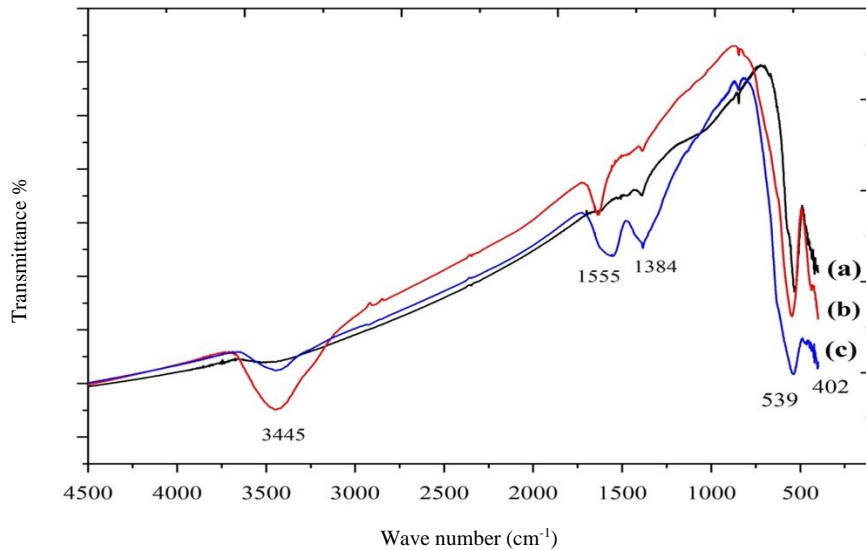


Fig. 3 - The FTIR spectrum of $\text{BiFe}_{1-x}\text{Zn}_x\text{O}_3$ nanocrystals: (a) $x = 0$; (b) $x = 0.06$; and (c) $x = 0.12$

3.3 The Magnetic Properties

The magnetic loop hysteresis on $\text{BiFe}_{1-x}\text{Zn}_x\text{O}_3$ ($x = 0, 0.06, \text{ and } 0.12$) were measured by VSM at room temperature (300 K) as shown in Fig. 4 and loop hysteresis of Bismuth ferrite shows a ferromagnetic phenomenon [14]. The VSM test shows that the ferromagnetic properties of $\text{BiFe}_{1-x}\text{Zn}_x\text{O}_3$ ($x = 0, 0.06, \text{ and } 0.12$) were decreasing because the loop hysteresis in the M-H curve of this materials were decreasing as well. As a result of the giving of Zn doping, with a concentration at $x = 0.12$, the value of magnetic saturation (M_s) was reduced by 2.81 emu/g , the magnetic remanent (M_r) was reduced by 0.22 emu/g , and magnetic coercivity (H_c) was decreased by 0.0007 T. The decreased magnetic saturation value of zinc doped BiFeO_3 were caused by the emergence of magnetic dipole moment of Zn^{2+} ion (diamagnetic) due to the magnetic field from the opposite direction and Zn^{2+} ions have substituted Fe^{3+} (ferromagnetic) caused the decreasing of magnetic dipole moment of Fe which totally reduces the magnetic dipole moment of BiFeO_3 . Table 2 also shows that $\text{BiFe}_{1-x}\text{Zn}_x\text{O}_3$ ($x = 0, 0.06, \text{ and } 0.12$) have a quite small coercivity field value (H_c) below 1 kA/m (0.0123 T) so that this material become a soft magnetic material. It can be concluded that due to the giving of zinc doping on BiFeO_3 material, the ferromagnetic characteristic reduced and potentially change to paramagnetic characteristic if the addition of zinc doping was increased.

Table 2 - The magnetic parameters of $\text{BiFe}_{1-x}\text{Zn}_x\text{O}_3$ nanocrystals ($x = 0, 0.06, \text{ and } 0.12$)

Samples	M_s (emu/g)	M_r (emu/g)	H_c (T)
$x = 0$	3.04	0.26	0.0013
$x = 0.06$	0.92	0.09	0.0011
$x = 0.12$	0.39	0.07	0.0009

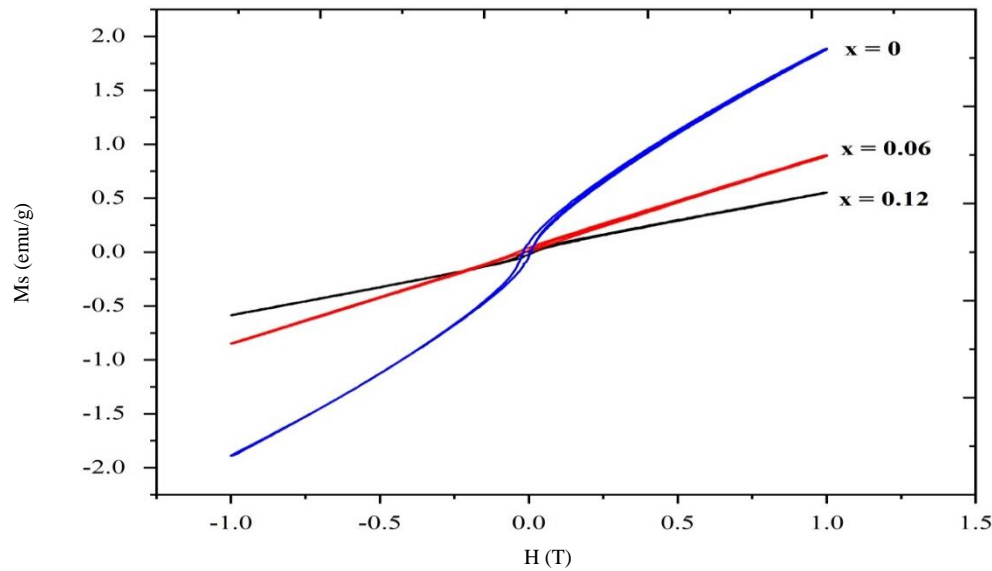


Fig. 4 - The Ms-H curve of BiFe_{1-x}Zn_xO₃ nanocrystals (x = 0, 0.06, and 0.12)

3.4 The Microwave Absorption Properties

The addition of zinc into BiFeO₃ nanoparticles through Fe anion substitution aims to give contribution on a better microwave absorbing characteristic. The Table 3 and Fig. 5 show the reflection loss (RL) of samples toward frequency (X band, 8.2 –12.4 GHz). From Fig. 5, it was observed that BiFeO₃ with zinc doping has better microwave absorption properties than BiFeO₃ without zinc doping. This was due to the contribution of bismuth ferrite magnetic properties which was greater. The bismuth ferrite with doping has RL of -25.79 dB at a frequency of 9.25 GHz and the zinc doped bismuth ferrite on x = 0.12 has RL of -30.02 dB at a frequency of 9.74 GHz. The good microwave absorption properties were always related to the high absorption conditions of a material. In general, the absorption rate of a material is expressed by the dielectric loss tangent (tan δ_e) and the magnetic loss tangent (tan δ_m) in Eq. (3) and Eq. (4).

$$\tan \delta_e = \frac{\epsilon''}{\epsilon'} \quad (\text{Dielectric loss tangent}) \quad (3)$$

$$\tan \delta_m = \frac{\mu''}{\mu'} \quad (\text{Magnetic loss tangent}) \quad (4)$$

Table 3 - The reflection loss (RL) of BiFe_{1-x}Zn_xO₃ nanocrystals (x = 0, 0.06, and 0.12)

Samples	Reflection loss (dB)	Frequency (GHz)
x = 0	-25.79	9.25
x = 0.06	-27.76	9.59
x = 0.12	-30.02	9.74

This suggests that the role of dielectric loss was greater than the effect of magnetic loss value. This was because the role of dielectric loss was influenced by the value of the dielectric constant, which means that the electrical properties are more dominant. The large dielectric loss contributes to the decreasing of reflection loss but also to a widening of the resonant frequency and the large dielectric loss causes the decreasing of the absorber impedance and the smaller absorber impedance obtains the smaller value of reflection loss (RL) [9].

$$Z_{RAM} = \sqrt{\frac{\mu_r}{\epsilon_r} \tanh \left(j \frac{2\pi f d}{c} \sqrt{\mu_r \epsilon_r} \right)} \quad (5)$$

$$RL \text{ (dB)} = 20 \text{ Log} \left| \frac{Z_{RAM} - 1}{Z_{RAM} + 1} \right| \quad (6)$$

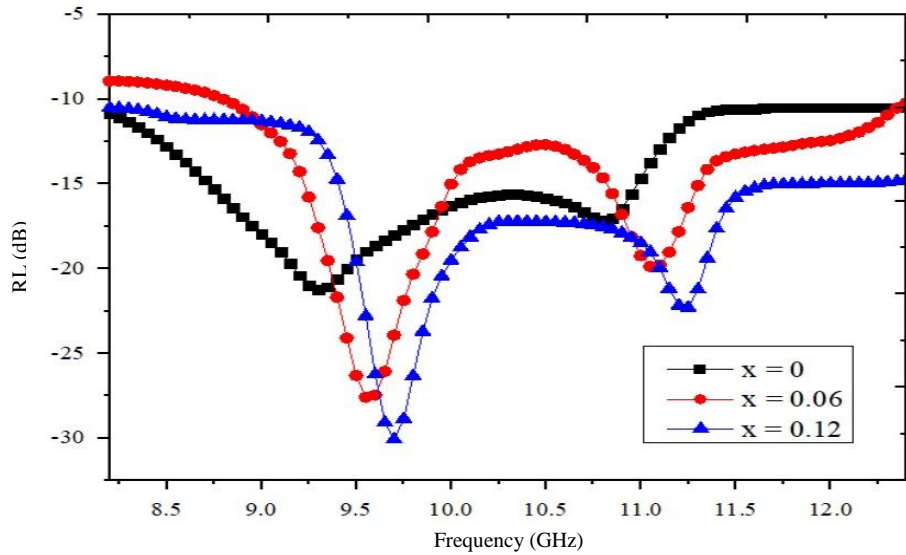


Fig. 5 - The reflection loss (RL) curve of $\text{BiFe}_{1-x}\text{Zn}_x\text{O}_3$ nanocrystals ($x = 0, 0.06,$ and 0.12)

The Fig. 6 show the magnetic loss and dielectric loss which contribute to the decreasing of the value of reflection loss (RL). In bismuth ferrite nanoparticles, the role of the dielectric loss gives a greater contribution than the value of magnetic loss in producing a smaller reflection loss. It can be concluded that the bismuth ferrite without doping has a reflection loss (RL) of -25.79 dB with a narrower frequency range and zinc doped BiFeO_3 has a RL of -30.02 dB with a wider frequency range.

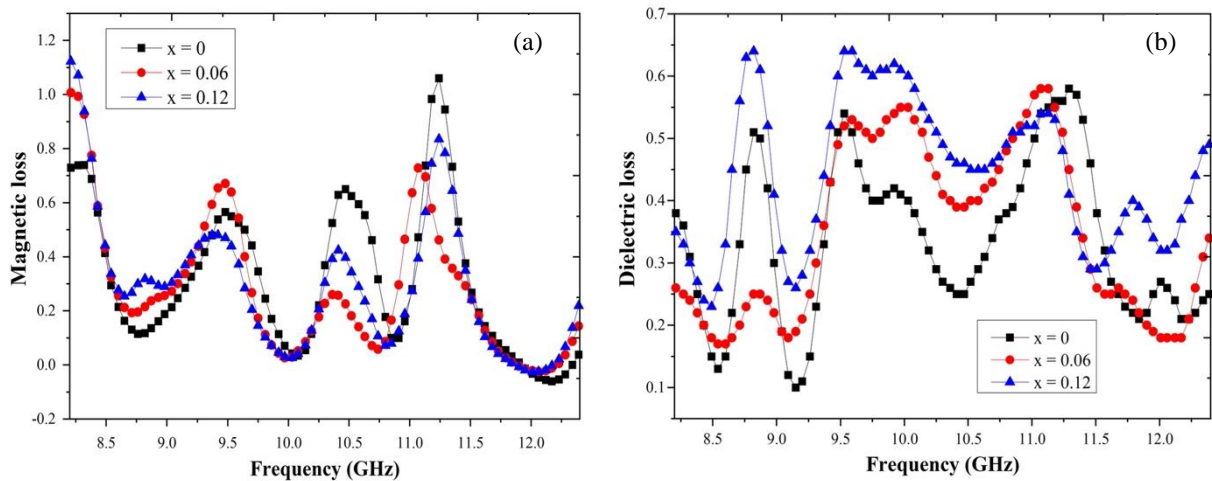


Fig. 6 - The curve of: (a) magnetic loss; (b) dielectric loss of $\text{BiFe}_{1-x}\text{Zn}_x\text{O}_3$ nanocrystals ($x = 0, 0.06,$ and 0.12)

4. Conclusion

The synthesis of zinc doped bismuth ferrite (BiFeO_3) have been successfully observed with sol-gel combustion method. The $\text{BiFe}_{1-x}\text{Zn}_x\text{O}_3$ nanoparticles ($x = 0, 0.06,$ and 0.12) have a rhombohedral structure and the ferromagnetic characteristic, however, increasing the doping concentration of Zn has an impact on decreasing the ferromagnetic properties and potentially the paramagnetic properties. The bismuth ferrite without doping has a RL of -25.79 dB with a narrower frequency range and bismuth ferrite with zinc doping has a RL of -30.02 dB so that bismuth ferrite with zinc doping have the potential to be a good absorbent material.

Acknowledgment

This research was conducted with an agreement contract between the author and the chairman of LPPMP Universitas Sebelas Maret Surakarta with contract number 124/UN27.21/HK/2020 through an independent research scheme.

References

- [1] Anon, (2016). Hybrid microwave absorbers. *Microwave Absorbing Materials*, 189–272.
- [2] Basantakumar, S. H., (2017). Multiferroic bismuth ferrite thin film and bismuth ferrite-cobalt ferrite nanocomposites. *Ferroelectrics*, 516(1), 90–97.
- [3] Wu, J. (2016). Multiferroic bismuth ferrite-based materials for multifunctional applications: Ceramic bulks, thin films and nanostructures. *Progress in Materials Science*, 84, 335–402.
- [4] Kong, L. B., Liu, L., Yang, Z., Li, S., Zhang, T., & Wang, C. (2018). Ferrite-based composites for microwave absorbing applications. *Magnetic, Ferroelectric, and Multiferroic Metal Oxides*, 361–385.
- [5] Peng, W., Howe, B., & Yang, X., (2019). Multiferroic RF/microwave devices. *Integrated Multiferroic Heterostructures and Applications*, 157–174.
- [6] Sharma, V., Rani, P., & K. Kunar, B. (2016). Multiferroic based microwave devices. *Advanced Materials Proceedings*, 1(1), 65–70.
- [7] Cheng, Y., & Ren, X. (2016). Enhanced microwave absorbing properties of La³⁺ substituting Barium Hexaferrite. *Journal of Superconductivity and Novel Magnetism*, 29(3), 803–808.
- [8] Zou, T., Wu, Y., & Li, H., (2018). Electromagnetic and microwave absorbing properties of carbon-encapsulated cobalt nanoparticles. *Materials Letters*, 214, 280–282.
- [9] Sun, J., Wang, Y., Wang, W., Wang, K., & Lu, J. (2018). Application of featured microwave-metal discharge for the fabrication of well-graphitized carbon-encapsulated Fe nanoparticles for enhancing microwave absorption efficiency. *Fuel*, 233, 6669–6676.
- [10] Zhang, F., Zeng, X., Bi, D., Guo, K., Yao, Y., & Lu, S. (2018). Dielectric, ferroelectric, and magnetic properties of Sm-doped BiFeO₃ ceramics prepared by a modified solid-state-reaction method. *Materials*, 11(11), 1–15.
- [11] Li, Y., Cao, W. Q., Yuan, J., Wang, D. W., & Cao, M. S. (2015). Nd doping of bismuth ferrite to tune electromagnetic properties and increase microwave absorption by magnetic–dielectric synergy. *Journal of Materials Chemistry C*, 3(36), 9276–9282.
- [12] Maran, R., Yasui, S., Eliseev, E., Morozovska, A., Funakubo, H., Takeuchi, I., et al. (2016). Enhancement of dielectric properties in epitaxial bismuth ferrite-bismuth samarium ferrite superlattices. *Advanced Electronic Materials*, 2(8), 1–9.
- [13] Musavi, G. S. E., Larki, M. R. & Kazeminezhad, I. (2020). The effect of Mn doped on the structural, magnetic, dielectric and optical properties of bismuth ferrite (BiFe_{1-x}MnxO₃) nanoparticles. *Vacuum*, 173, 1–31.
- [14] You, S. & Zhang, B. (2020). Enhanced magnetic properties of cobalt-doped bismuth ferrite nanofibers. *Materials Research Express*, 7(4), 1–8.